Journal of Casting & Materials Engineering Vol. 6 No. 4 (2022) 81–92
https://doi.org/10.7494/jcme.2022.6.4.81

The Formation, Properties and Use of Dispersed Iron-Graphite Metallurgical Waste

Leonid Dan[a*], Vladimir Maslov[b], Larysa Trofimova[b], Grzegorz Cios[a]

[a] AGH University of Science and Technology, Academic Centre for Materials and Nanotechnology, al. A. Mickiewicza 30, 30-059, Krakow, Poland
[b] Priazovskyi State Technical University, Faculty of Metallurgy, Dmytro Yavornytsky, Av. 19, 49005, Dnipro, Ukraine
e-mail: danleonid.alex@gmail.com

Received: 26 September 2022/Accepted: 13 November 2022/Published online: 30 December 2022.
This article is published with open access at AGH University of Science and Technology Journals.

Abstract

Dispersed wastes containing graphite, iron, and its oxides, getting into the air and accumulating in landfills, cause serious harm to human health and the environment. Moreover, even if the issue of the localization of these wastes has been solved successfully, their disposal has not yet been fully organized. In the present study, a systematic analysis of the dispersed iron-graphite waste (IGW) conditions for the formation at metallurgical enterprises, their structure, and their properties were carried out. In this case, special attention is focused on the electrophysical properties: specific saturation magnetization and volume resistivity. The presence of magnetic properties in IGW, combined with low electrical resistivity, makes IGW a promising and inexpensive raw material for obtaining cheap composite materials with radio shielding and radio absorbing properties in the microwave range. As a result of the research, effective ways of improving the magnetic properties of IGW by high-temperature treatment were obtained. The practical result of the research was the development and implementation of a technological scheme of dispersed IGW complex processing, which makes it possible to solve a twofold task – to exclude the ingress of iron-graphite wastes into the environment and to obtain a cheap material for protection against microwave radiation.

Keywords:

dispersed iron-graphite waste, graphite, iron oxides, specific saturation magnetization, magnetizing annealing, carbothermal self-reduction, magnetic graphite

1. INTRODUCTION

The metallurgical industry occupies one of the leading places regarding the degree of negative environmental impact. The reduction of greenhouse gas emissions by metallurgical enterprises is one of the main problems which the efforts of scientists and engineers are currently focused [1]. At the same time, attention is being drawn to the fact that in the production of 1 ton of cast iron, up to 600 g of waste containing graphite and iron oxides – iron-graphite waste is emitted [2]. Global practices show that iron-graphite waste can be used in metallurgy and in many other industries [3–7]. Technologies that make it possible to extract only the graphite component of IGW prevail, while the remainder is turned into waste again. This is unacceptable from an environmental point of view and irrational from the economic perspective because, in addition to graphite, the composition of IGW includes valuable components – iron oxides and metallic iron.

Therefore, the solution to issues related to the search for new IGW complex processing technologies, expanding the scope of their application, meets, on the one hand, the requirements of environmental protection and, on the other hand, allows for the more efficient use of valuable raw materials.

2. CONDITIONS FOR THE FORMATION OF DISPERSED IGW AT METALLURGICAL ENTERPRISES

Iron-graphite wastes have different compositions, structures, and properties depending on the formation at metallurgical enterprises.

Dispersed IGW is essentially graphite dust (kish graphite together with the tiniest splashes of cast iron and slag released into the atmosphere during the pouring and desulphurization of liquid iron), which is collected by aspiration systems.

The formation of graphite dust is explained [8, 9] by the dissolution of cementite in austenite and its dissociation into Fe and C as the cast iron cools when it leaves the furnace. In this case, the solution of carbon in iron becomes supersaturated,

which leads to the formation of graphite nuclei and their further intensive growth. Furthermore, the density of graphite is 2–2.5 times less than the density of metal, so the metal tends to push the plates to the surface, and since the metal does not wet them, they are freely blown away from the surface by the gas flow. In this regard, graphite dust is formed with any increase in the open (specific) surface of the metal, for example, during overflows or during its transportation through chutes. The solubility of carbon in an iron-carbon melt (Eq. (1)) and in real cast iron containing silicon and other elements (Eq. (2)) is expressed, respectively, by temperature dependences based on empirical formulas [8]:

$$C_1'=1.30+2.57^{-3}t \quad (1)$$

$$C_1 = 1.27 + 2.57 \cdot 10^{-3} t - 0.34\text{Si} \quad (2)$$

where:

t – temperature, °C;
C_1', C_2 – carbon content, %.

Thus, the more supercooled the metal, the more carbon there is in the form of graphite inclusions, and the more dust is formed. As the established practice of metallurgical plants confirms, liquid iron in iron ladles cools down at a rate of 3–6 deg/h, while an open jet cools down by approximately 30 degrees in a matter of minutes [9]. During the period from the release from the blast furnace and transportation to the mixer, the temperature of the cast iron decreases by 130–180°, which naturally leads to a significant extraction of graphite from the cast iron. It was shown in [10] that graphite precipitation does not occur in the volume of cast iron but on the interfacial surfaces: exposed metal surface in the ladle, melt-ladle wall, and melt-gas bubble. When cast iron is poured into the mixer and then into the ladle, partial spraying and gas capture by the jet occurs. The resulting gas bubbles penetrate the liquid iron layer, which leads to a sharp increase in the iron-gas interface. This significantly reduces the energy of formation and growth of graphite nuclei. As a result, the number of graphite particles becomes significantly more significant, and their size is smaller than when downloading slag.

From this point of view, in the desulfurization section, the conditions for the formation and separation of graphite from cast iron are even more favorable since this process involves purging the cast iron with air, nitrogen, or rock gas (at a flow rate of up to 100 m^3/h).

Various impurities in the metal have different effects on the process of graphite formation and, consequently, on dust formation. For example, Cr, Mn, S, and Mg hinder graphite formation, while Si, on the contrary, enhances this process and increases the amount of dust [4].

3. MATERIALS AND METHODS

Systematic studies of the IGW of the mixing department and the desulfurization department of the oxygen-converter shop of Azovstal Iron and Steel Works (Mariupol, Ukraine) were carried out.

For this, samples were taken (weight 2 kg) from the bins of the aspiration system. The samples were then averaged over 1 hour in a cone mixer. Next, to conduct property studies, the samples were reduced by quartering to obtain representative batches (0.5 kg). Finally, samples were taken from each batch for all subsequent analyzes and studies.

Comprehensive IGW properties studies included: a) chemical analysis; b) granulometric analysis; c) study of the microstructure; d) study of the specific volume electrical resistance, ρ_v; e) measurement of the specific saturation magnetization, σ_S.

The microstructure and morphology of IGW particles were studied using a Neophot-30 optical microscope; a REM scanning electron microscope with an X-ray analyzer and a JEM transmission electron microscope were also employed.

The differential thermal analysis method was applied to determine the temperatures of phase transformations in the studied IGW.

The magnetic properties were studied according to the procedure described in [11] using a specially made device.

To study the possibility of increasing the level of magnetic properties by their heat treatment, the installation shown in Figure 1 was used. The installation made it possible to process the material in a fixed layer and under the following modes of motion: a) a dense moving layer; b) a gravity-falling layer; c) a combined layer – gravitationally falling with subsequent movement in a dense layer.

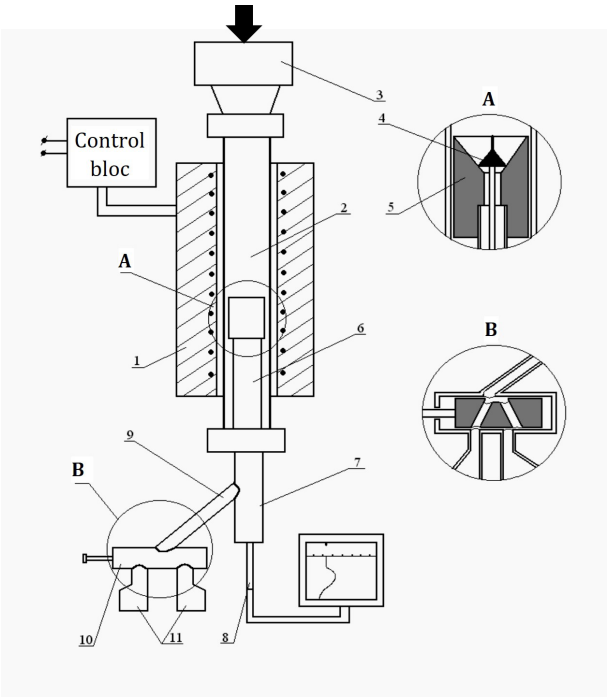

Fig. 1. The laboratory installation for heat treatment of IGW: 1 – furnace; 2 – reactor; 3 – loading device; 4 – cone; 5 – cup; 6 – tube; 7 – reactor; 8 – rod; 9 – chute; 10 – switch; 11 – material receivers

The installation consisted of an electric furnace (1) with a reactor (2) made of quartz glass. The upper part of the reactor was connected to the loading device (3), which allowed it to load dispersed IGW into the reactor without breaking the tightness. A graphite cup (5) with a cone (4) were installed in

the reactor to accumulate the material. The shutter was fixed on a tube (6), transporting the sample to the receiver. With the help of the rod (8), it was possible to move the shutter along the reactor, thereby regulating the processing time of the material while moving along the reactor.

The lower part of reactor (7) was connected to an unloading device consisting of a chute (9), a spool-type flow direction switch (10), and material receivers (11). Depending on the position of the switch, the sample entered one or another receiver without leakage. This installation also allowed conducting experiments in a controlled CO-CO_2 atmosphere in the reactor.

4. EXPERIMENTAL RESULTS AND DISCUSSION

4.1. Chemical composition

In the study of the chemical composition of dispersed IGW, the content of Fe_{met}, FeO, Fe_2O_3, C, and impurities was determined. Figure 2 shows the averaged data on the chemical composition of the IGW of the mixing department and of the desulfurization department.

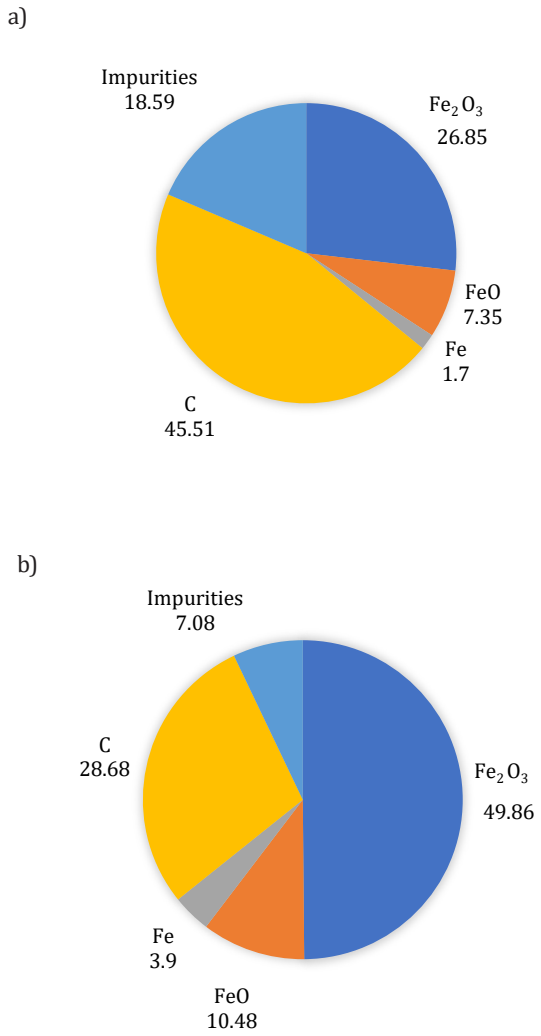

Fig. 2. The average chemical composition [%] of dispersed IGW of the desulfurization (a) and mixing (b) departments, based on [12]

As shown in Figure 2, the most typical results of the chemical analysis of the initial dispersed IGW show that the composition of these wastes depends significantly on the sampling place. For example, lower carbon content is observed in samples of the mixing department (average value – 28.68%, minimum – 14.56%, maximum – 38.44%) compared with samples of the desulfurization departments. At the same time, a higher content of iron oxides is observed (FeO, respectively, average, minimum and maximum values: 10.48, 7.57, and 15.16%; for Fe_2O_3, respectively: 49.86, 34.07, and 70.98%). Almost all of the samples contain a small amount of metallic iron, which enters the dispersed IGW in the form of tiny splashes of cast iron when poured into a mixer or a ladle (for samples from the mixing department: 3.9, 0.79 and 9.32%, respectively).

As shown, dispersed IGW in the desulfurization department is formed under somewhat different conditions, namely, when liquid iron is blown with an inert gas and magnesium powder. In this case, the cooling rate of liquid iron is greater than in the previous case, and consequently, the release of graphite is more intense. Dispersed IGW of the desulfurization department contain more carbon (average value 45.51%, minimum – 36.15%, maximum – 53.23%). According to metallic iron content, these two types of waste are close, but for the mixing department, the upper limit of the Fe_{met} content is significantly higher than for the desulfurization department (respectively, 1.7, 0.0, and 4.73%). The content of oxides for the desulfurization department IGW is less than for the mixing department (FeO, respectively, the average, minimum and maximum values: 7.35, 5.38, and 12.35%; for Fe_2O_3, respectively: 26.85, 15.51 and 34.03%).

4.2. Particle size distribution

The results of the sieve analysis of the samples of the mixing department IGW and the desulfurization department show that the central part of the material has a fineness of less than 400 μm (Fig. 3). Furthermore, a comparison of the averaged curves for the desulfurization department and the mixer department showed that the regularities of the distribution of IGW particles by fractions are universal for all the studied samples.

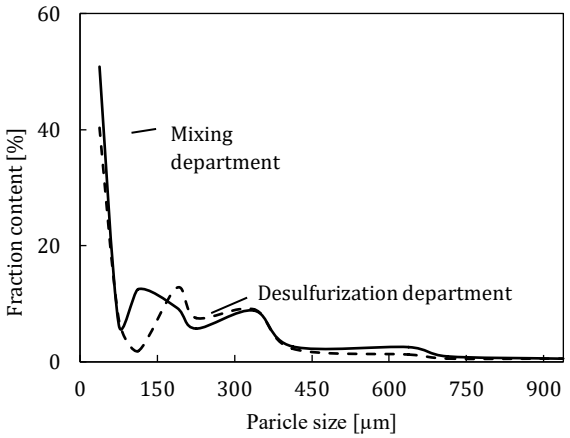

Fig. 3. Size distribution of IGW particles

Tables 1 and 2 show, by way of examples, the content of the components in various fractions of IGW for a sample from the desulfurization department. An analysis of the distribution of the main components of IGW by fractions showed the following: with a decrease in particle size, the carbon content decreases from 85% for a fraction of (−1000 +200) μm to 7.3% for a fraction of less than 50 μm. The material remaining on the sieve is marked with a plus (+) sign, and the material that has passed through the sieve is marked with a minus (−) sign. The content of FeO increases from 3.12% for the fraction (−1000 +200) μm to 16.02% for the fraction (−100 +63) μm. For the fraction −50 μm, the content of FeO is 15.46%. The content of Fe_2O_3 increased monotonically with decreasing particle size from 4% for the fraction (−1000 +200) μm to 63.3% for the fraction less than 50 μm. The amount of Fe_3O_4 with decreasing particle size increased from 11% for the fraction (−200 +160) μm to 42% for the fraction less than 50 μm.

Table 1
The main components content of the IGW depending on its dispersion (desulphurization department)

Fraction size [μm]	Chemical composition [%]				
	C	Fe_{Σ}	$Fe_{met.}$	FeO	Fe_2O_3
Polydisperse material	53.35	29.03	4.73	9.70	23.90
+1000	87.50	3.15	3.15	–	–
−1000 +200	85.00	8.00	2.76	3.12	4.0
−200 +160	74.00	10.74	5.52	6.85	–
−160 +100	71.23	15.00	5.50	7.00	5.70
−100 +63	48.50	31.63	13.80	16.02	7.61
−63 +50	28.50	41.03	10.65	5.30	37.50
−50	7.30	60.25	3.95	15.46	63.30

Table 2
Impurity content of the IGW depending on its dispersion (desulphurization department)

Fraction size [μm]	Chemical composition [%]						
	SiO_2	Al_2O_3	CaO	MgO	MnO	P_2O_5	S
Polydisperse material	2.10	1.10	2.90	1.00	0.90	0.474	0.231
+1000	0.72	1.01	1.86	0.22	0.90	0.948	0.112
−1000 +200	0.80	1.10	2.00	0.45	1.10	0.474	0.155
−200 +160	3.12	1.16	3.72	0.90	1.29	0.379	0.320
−160 +100	4.00	1.10	3.50	1.39	1.00	0.758	0.369
−100 +63	4.00	1.45	3.41	1.79	0.90	0.568	0.369
−63 +50	3.90	1.40	3.20	2.01	1.05	0.568	0.330
−50	2.40	0.90	3.00	1.20	1.05	0.474	0.129

4.3. Morphology and microstructure of the initial dispersed IGW particles

Figure 4 shows a general view of a layer of graphite particles and elements of the surface of a graphite plate of the IGW obtained on a scanning electron microscope. Point formations are visible on the surface of the particle. Their number corresponds to the carbon content in the IGW sample.

Increasing the magnification made it possible to detail these formations. At the same time, it was possible to determine the diameter of spherical oxide formations (from 1–5 to 25–35 μm). The level of the magnetic properties of the dispersed IGW is closely related to the amount of oxide inclusions on the surface of a graphite plates.

The use of a transmission electron microscope made it possible to establish the nature of the mutual distribution of graphite and oxide particles (Fig. 5). On Figure 5a traces of delamination of the end face of the graphite plate are visible.

There are spherical oxide particles in the protruding graphite element. They have a diameter of 250–2200 Å. Oxide particles are firmly connected with graphite, some are completely in the body of the graphite plate.

Figure 5b shows the formation of oxide particles located on the surface of a graphite plate, in which a large particle with a diameter of 1.45 μm is tightly connected to a smaller one, having a diameter of 0.43 μm. Even smaller particles are also visible, covering the surface of a larger one with a diameter of 10 to 100 nm.

The structure of the oxide particle shown in Figure 6a is also characteristic. The particle is a dense formation with a diameter of 160–170 μm, consisting of sintered smaller particles. From the outside, the shell of the particle resembles an "orange peel" type structure. The internal volume is filled with minor oxide spherical particles with a diameter of 2–10 μm. Small particles 2–7 μm in diameter are visible on the outer the surface of this large spherical object.

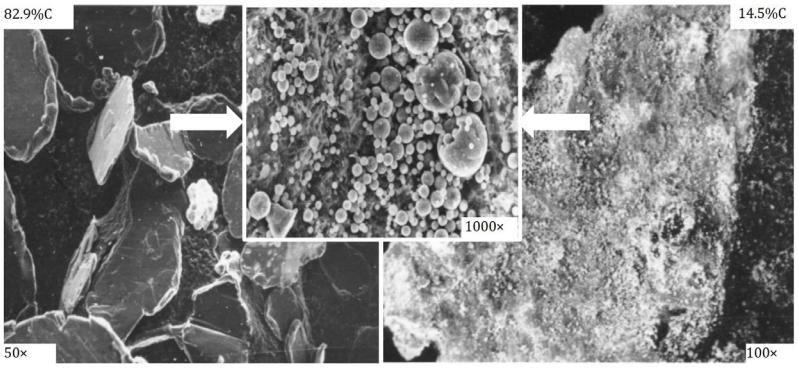

Fig. 4. Microstructure of the graphite plate surface, based on [13]

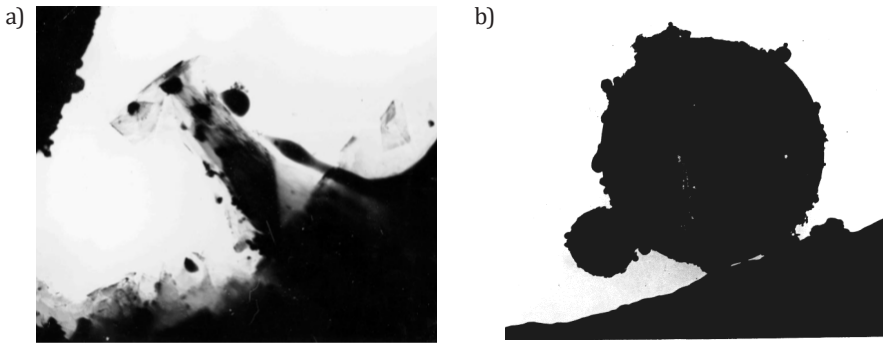

Fig. 5. Fragments of the surface of IGW graphite plates: a) graphite plate end; b) graphite plate surface, based on [13] 40 000×

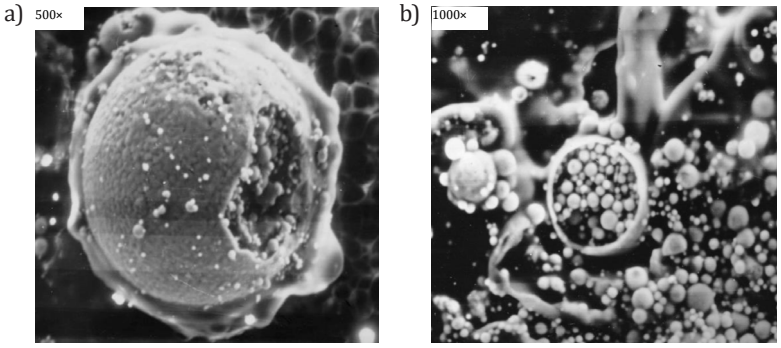

Fig. 6. . Structure of oxide particles: a) "orange peel" type structure; b) sample preliminarily subjected to pressure treatment, based on [13]

Additional information about the structure of the oxide particles of IGW is provided by the study of IGW samples preliminarily subjected to pressure treatment (in this case, a sample of the studied material was scattered on a matrix plate, and pressure was applied from above with a punch). The fracture structure (Fig. 6b) indicates that in some cases the particle is a shell filled with spherical oxide inclusions from 1 to 10 μm in diameter.

So, the study of the morphology of the initial dispersed IGW showed that they are graphite particles, the surface of which is covered to a greater or lesser extent by oxide inclusions having a complex structure. In one case, these are particles primarily of smelting origin representing dense oxide formations. In another case, these are particles that are a conglomerate of intergrown particles of smaller size, which were longer in the high-temperature zone, and this led to their strong diffusion intergrowth.

Graphite particles had a lamellar elongated shape with a thickness from 3–4 to 80 μm a characteristic luster and a layered structure. In the vast majority of particles, there were inclusions of metal directly into the body of graphite plates (Fig. 7).

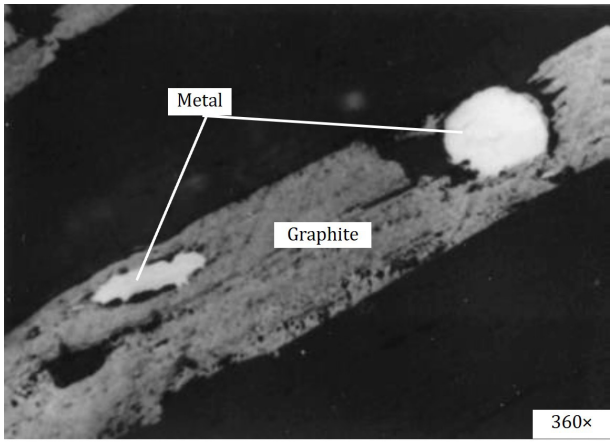

Fig. 7. Microstructure of IGW graphite particles, based on [13]

The microstructure of metal particles is carbide plates with colonies of ledeburite. This is due to the high cooling rates of metal particles in the gas flow that captured them during dispersion.

4.4. Electrical and physical properties

The specific saturation magnetization (σ_s) and electrical resistivity (ρ_v) are the most critical electrophysical properties of dispersed IGW. Therefore, the analysis of these properties of the studied materials was carried out depending on various parameters.

It is known from the literature [14–16] that dispersed IGW have magnetic properties. However, they vary widely (σ_s = 22–45 A·m^2/kg).

Figure 8 shows the relationship between the granulometric composition of dispersed IGW and its magnetic properties. In the experiment, it was found that with a decrease in the dispersion of the material, the value of σ_s increases and reaches a maximum for the tiniest fractions. The maximum of σ_s with a simultaneous minimum of $Fe_{met.}$ (Tab. 1) makes possible the conclusion that the oxide magnetic component plays a dominant role in the magnitude of the magnetic properties. Dispersed IGW, as a rule, have a very low electrical resistivity – (4.18–0.46)·10^{-4} ohm·m [16]. Since dispersed IGW are polydisperse, a study was made of the effect of the dispersed composition on the specific electrical resistance. The ρ_v of the starting material is 2.41·10^{-4} ohm·m. The results of measuring ρ_v of individual fractions are shown in Figure 9. For ease of perception, the dependence of ρ_v on the particle size in Figure 9 was built in semi-logarithmic coordinates.

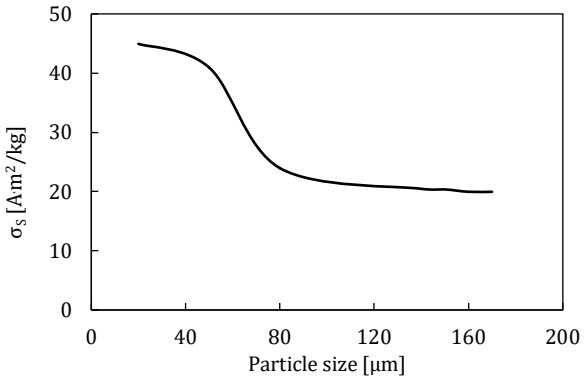

Fig. 8. Dependence of the magnetic properties of dispersed IGW on the granulometric composition

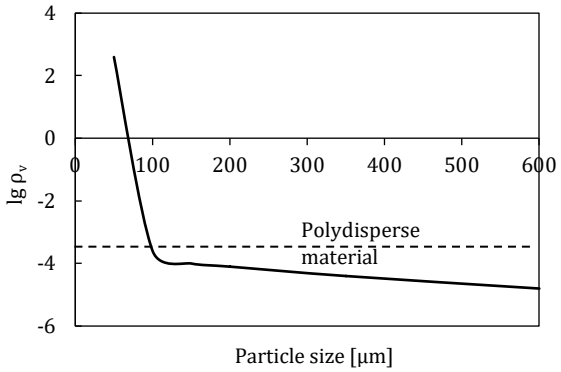

Fig. 9. Specific electrical resistance of IGW depending on their dispersion

Analysis of the graph shows that in the range from 600 μm to 200 μm, the value of ρ_v is minimal and lies within (2.06–2.53)·10^{-4} ohm·m. In the dispersity range of 200–63 μm, an increase in ρ_v from 2.25·10^{-4} to 6.0·10^{-4} ohm·m is observed with a decrease in particle size, which is due to a decrease in the carbon content from 28.0 to 8–15%. A further decrease in dispersion leads to an even greater decrease in the carbon content. As a result, already for a dispersion of 50–63 μm, the value of ρ_v is 0.15·10^{-2} ohm·m, and for a dispersion of less than 50 μm, the value of ρ_v becomes equal to ~5·10^3 ohm·m. Thus, the value of ρ_v, depending on the disperse composition, can vary by almost six orders of magnitude.

4.5. Differential thermal analysis of IGW

The chemical composition and morphology of dispersed IGW in the context of their magnetic properties showed that the

material has excellent potential for these properties. An increase in the content of magnetic components (metallic iron and Fe_3O_4 oxide) in IGW is possible due to carbothermal self-reduction in the first case and magnetizing annealing in the second.

When studying reduction processes in new systems, it is essential to determine the temperatures at which the interaction begins [17]. For this purpose, a differential thermal analysis (DTA) of the studied dispersed IGW was carried out.

DTA was carried out stepwise: heating at a rate of 10 degrees per minute to a temperature of 850°C and then at a rate of 2 degrees per minute.

The results obtained show that there are three segments on the DTA curve. The first endoeffect was observed at temperatures of 60–200°C. In this case, condensation of water droplets was observed on the cold parts of the reactor with the sample. Thus, the first peak of the endoeffect corresponded to the removal of hygroscopic moisture from the sample.

The endoeffect was observed at 500–850°C, a more petite height but extended in time. At the same time, a slight gas evolution occurred in the reactor.

An additional experiment carried out at 900°C, and a long exposure showed that a non-magnetic material is obtained at this temperature, i.e., all iron oxides are converted to wustite. Consequently, the peaks corresponding to the reduction of hematite and magnetite on the thermogram merge into one peak. This was due to the high heating rate at this analysis stage.

The third peak of the endoeffect began at 960 ±5°C and was accompanied by the greatest of the endoeffects. From this moment, intensive gas evolution began. This DTA peak is a consequence of the endoeffect of reduction of wustite by the graphite. With an increase in temperature, the intensity of gas evolution increased, and the magnitude of the endoeffect grew. The limiting temperature during thermographic studies was 1000°C.

The analysis of the obtained results showed that the magnetizing treatment of dispersed IGW should be carried out in the temperature range of 600–700°C and metallization – at temperatures above 980°C.

4.6. High-temperature treatment of dispersed IGW

Magnetizing annealing

The conditions for carrying out the technological process of high-temperature treatment of dispersed IGW determine the quantitative characteristics of the process, as well as the parameters of the resulting product. In this regard, the following options for the implementation of magnetizing annealing and carbothermal self-reduction were investigated in this work: a) in a dense fixed layer; b) in a dense vertically moving layer; c) in a combined (gravitationally falling and following a dense moving) layer.

When choosing the operating temperature range, we were guided both by the DTA results and by the course of the curves on the Fe-O-C equilibrium diagram. The lower temperature limit at which magnetite becomes a thermodynamically probable phase is 570°C. At temperatures above 650°C, wustite becomes more thermodynamically probable [18–21].

According to [22], in the case of carbon content in ores of more than 0.1%, it is sufficient to heat the ore to 570–660°C to carry out magnetizing annealing without using a reducing agent. Moreover, if it is necessary to use the reducing effect of the carbon in the ore, then the ore heating in the furnace is recommended to be carried out in a neutral atmosphere or without air access. Solid carbon reduces the ore only at a temperature of approximately 650°C [22, 23]. Based on this brief analysis, the following temperatures were chosen for the experiments: 600, 650, and 700°C.

The presence of such an amount of carbon in the material and oxygen in the reactor of the installation provided the necessary $CO\text{-}CO_2$ atmosphere for the reduction reactions to proceed in full. The material was heated and processed in a reactor (Fig. 1) without air access, i.e., in its atmosphere. The obtained results were analyzed only for the period of isothermal exposure to the material. During the experiments, the σ_s of the final product was controlled. Figure 10 shows the kinetic curves of the magnetizing annealing of these samples. At a process temperature of 600°C, an increase in the value of σ_s was observed with an increase in the isothermal holding time from 0 to 90 min, but the process was especially intensive in the first 10 min. The maximum value of σ_s was obtained only after 90 min of the experiment (75 min of exposure at a constant temperature) and amounted to 87 $A{\cdot}m^2/kg$ (or 94.5% of the maximum possible value corresponding to the content of 100% magnetite).

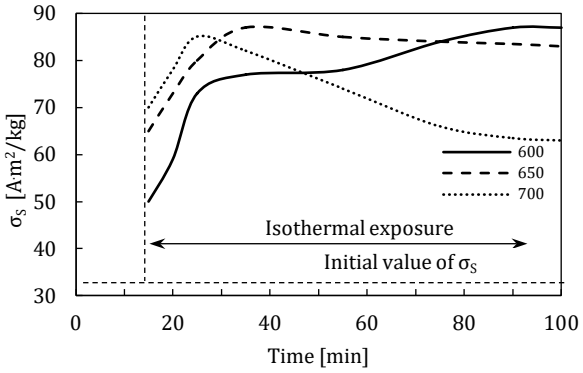

Fig. 10. Kinetics of magnetizing annealing of IGW in a dense fixed layer, based on [24]

Increasing the temperature to 650°C led to the intensification of the process. Thus, after 20 min of exposure at a constant temperature, the value of σ_s reached 87 $A{\cdot}m^2/kg$.

With a long exposure, the gas medium should approach equilibrium by the Fe-O-C diagram. According to this diagram, at temperatures above 650°C, the gas phase corresponds to the stable state of wustite. However, the process of magnetite formation is faster than its reduction to wustite. Therefore, at temperatures above 650°C, at first, most of the oxides are converted into magnetite, and with an increase in its amount, reduction to wustite begins. This explains the course of the curve at 700°C in Figure 10. From a technological point of view, the moving layer is more attractive than the fixed one. In experiments on magnetizing annealing in a dense moving layer, the speed of material movement through the reactor was 5, 10, 20, and 40 mm/min. At the

same time, the residence time of the material in the thermostable zone with a temperature of 650°C was 80, 40, 20 and 10 min, respectively.

Figure 11 shows the kinetic curve of the magnetizing annealing of the IGW in a dense moving layer. As in previous experiments, it was enough to keep the material at 650°C for 35 min to obtain 95% of magnetite from the maximum possible amount. This corresponded to the speed of movement of the material through the reactor, 10 mm/min.

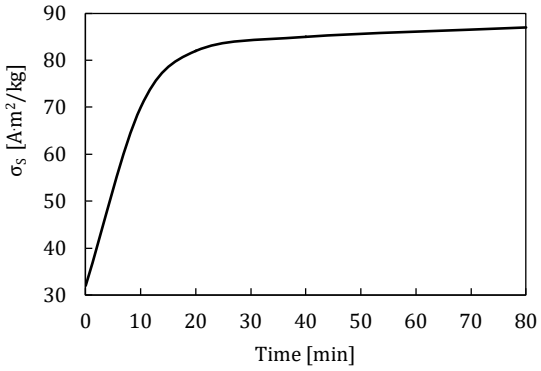

Fig. 11. Kinetics of magnetizing annealing of IGW at 650°C in a dense moving layer

The experiments have shown that obtaining high values of σ_s is associated with a long processing time. The link limiting the performance of the reactor is the rate of heating of the processed material to the operating temperature. A dense layer of IGW can be identified with a quasi-monolithic body, which has low thermal conductivity and warms up slowly. On the other hand, it is known that in the mode of a gravitationally falling layer, very high heat transfer coefficients can be obtained – up to 3000 W/(m²·K) [25].

The features of the gravitationally falling layer are as follows:

1) particles entering the reactor are in a state independent of each other and begin to move only under the action of gravitational force. When their movement conditions are met, heating, chemical, and structural transformations will be equivalent. In this case, the powder particles are accelerated to a speed equal to or close to the speed of hovering relative to the reagent gas. Heating and all transformations are thus carried out in the process of falling particles;
2) the distance between the particles significantly exceeds their diameter;
3) each particle is in an equiprobable state from the point of view of flow by the reagent gas and interaction with it.

Studies of the magnetizing annealing of dispersed IGW in their atmosphere (IGW carbon content – 10%) in the mode of a gravitationally falling layer, followed by exposure in a dense layer, were carried out on an installation, the scheme of which is shown in Figure 1. In the gravitational falling layer mode, the material passed through the non-isothermal zone of the reactor, was heated to the operating temperature, and then accumulated in the isothermal zone. The temperature in this reactor zone was set in the range from 600 to 800°C.

It was found that already after 2 seconds of movement in the falling layer mode, the saturation-specific magnetization increased from 32 to 47 A·m²/kg at a reactor temperature of 600°C, to 62 A·m²/kg at a reactor temperature of 650°C, to 70 A·m²/kg at a reactor temperature of 700°C and up to 75 A·m²/kg at a reactor temperature of 800°C.

Further exposure for 100 min at a temperature of 600°C led to a monotonic increase in the value of σ_s up to 87 A·m²/kg. This indicated the transition of almost all iron oxides contained in the samples to magnetite.

The process of magnetizing annealing at higher temperatures in a dense layer proceeded very quickly: at 800°C, an increase in the value of σ_S to 87 A·m²/kg was observed already after 2–3 min from the start of treatment, and at 700°C, after 7–8 min. Then, by the Fe-O-CO-CO_2 diagram, the transformation of the formed magnetite into the nonmagnetic oxide FeO began. This led to a decrease in the sample's magnetic properties to 60 A·m²/kg after 100 min exposure.

On the basis of the results obtained, it was proposed to preheat the initial dispersed IGW in the gravitational-falling layer mode before magnetizing annealing in the dense layer mode. Considering in addition to technological and economic aspects, the optimal temperature in the reactor should be recognized as 700°C.

Carbothermal self-reduction

Both magnetite and metallic iron can ensure the high magnetic properties of iron-graphite waste after high-temperature treatment. The process leading to the reduction of all iron oxides of IGW to metallic iron by the carbon contained in the material itself is, in fact, the process of carbothermal self-reduction (CTSR).

The studies were carried out on polydisperse samples of IGW with a fraction of fewer than 400 μm. The samples contained 38% C and ~40% Fe_{Σ}. In the experiments, the samples were heated in a dense fixed layer to 1000, 1025, and 1090°C. In the process, the degree of reduction, α, was determined.

Curves characterizing the kinetics of the process of CTSR of IGW to metallic iron (metallization) at given temperatures are shown in Figure 12.

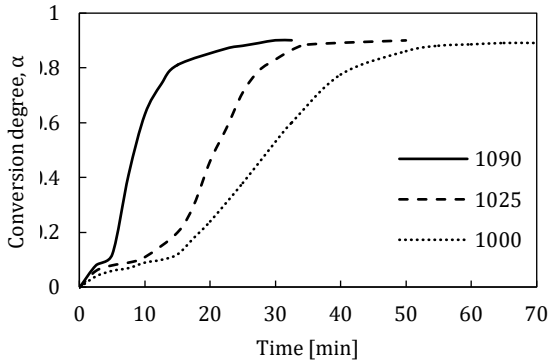

Fig. 12. Kinetics of CTSR of IGW in a dense fixed layer, based on [26]

It can be seen from the figure that the temperature significantly affects the total duration of reduction up to the value α equal to 0.9 (σ_s = 180 A·m²/kg). The temperature increasing from 1000 to 1090°C reduces the processing time

from 70 to 30 min, i.e. 2.33 times. The shape of the curves indicates a two-stage reduction process. It is thermodynamically apparent that the reduction of higher iron oxides to wustite took place in the first stage, and the process of metallization took place in the second stage. Both stages began very quickly in this case, then the process slowed (Fig. 12).

Consideration of each step of the process from the point of view of topokinetic theory made it possible to explain the course of the curves in Figure 12.

It is known that if a chemical process proceeds with the participation of different phases, the reaction occurs at their interface [27, 28]. Therefore, the process studied in this work is topochemical. Modern topochemistry considers such processes as two-stage ones [29]. The first stage of interaction between a gas and a solid consists of forming product nuclei on the surface of a solid reagent, their growth, and coalescence. In the second stage, a continuous thin shell of the product is formed on the entire reaction surface, followed by the advance of the reaction front deep into the solid reagent. In this case, the process rate decreases under the influence of two factors: a decrease in the reaction surface and an increase in the effect of diffusion resistance due to the layer of the solid product thickness increasing. In the study of processes in the combined mode of motion, a sample of dispersed IGW was heated in a gravitationally falling layer, then in a dense layer, iron oxides were reduced by the carbon of the sample. As in the case of magnetizing annealing, preheating of the material in the mode of a gravitationally falling layer significantly accelerated the process. Thus, at a temperature in the isothermal zone of 1090°C, the metallization process was completed by ~90% after 24 min, at a temperature of 1025°C – after 28, and at 1000°C – after 50 min, i.e. flowed approximately 1.23 times faster than in the dense layer regime.

4.7. General technological scheme of dispersed IGW processing

The complex studies conducted on the physicochemical, electrophysical, and technological properties, as well as their morphology and microstructure, allows us to consider dispersed IGW of metallurgical production as a promising raw material for creating composite materials with radio-absorbing and radio--shielding properties. This follows from the considerations below.

To create effective composite materials that absorb microwave radiation, it is necessary to be guided by physical and electrophysical concepts in combination with a physicochemical approach to finding optimal compositions. At the same time, a thorough analysis shows that one of the most promising ways is using heterogeneous two- or more-component materials.

The first essential physicochemical condition for the most efficient absorption of materials of the metal (oxide) – dielectric type of microwave radiation is the following: maximum absorption is achieved if the dimensions of the metal component are one order of magnitude or not more than one order of magnitude greater than the value of the skin layer, and a component with dielectric properties completely insulates a metal component evenly distributed over the volume.

The second physicochemical condition for creating materials that absorb microwave radiation is using such components with high structure stability, composition, and properties under thermal, corrosion, and other influences.

Based on these prerequisites and the generalization of the results obtained in laboratory studies, a general scheme of dispersed IGW complex processing was developed (Fig. 13). Considering the heterogeneity of IGW from various sources, both in terms of chemical and granulometric composition, in accordance with the proposed scheme, the waste should be subjected to screening, grinding, and averaging.

Based on the fact that the central part of iron oxides is contained in a fraction of less than 160 μm, and the main proportion of graphite is in a fraction of more than 160 μm (Tab. 1), it is proposed to divide the IGW into two fractions: +160 and –160 μm.

At the same time, the +160 μm fraction of IGW can be used directly without further processing, for example, as a raw material for graphite extraction. The –160 μm fraction has higher magnetic properties and can be used as a starting material for further high-temperature processing to increase the level of these properties. Stabilization of the properties of the starting material and the final product is ensured by averaging.

In order to obtain a fraction of IGW less than 50 μm, the technological scheme provides for a grinding operation, after which the resulting material (–50 μm) is also sent to an average.

An increase in the magnetic properties of iron-graphite waste is associated with the screening of a large fraction and with the implementation of high-temperature processing.

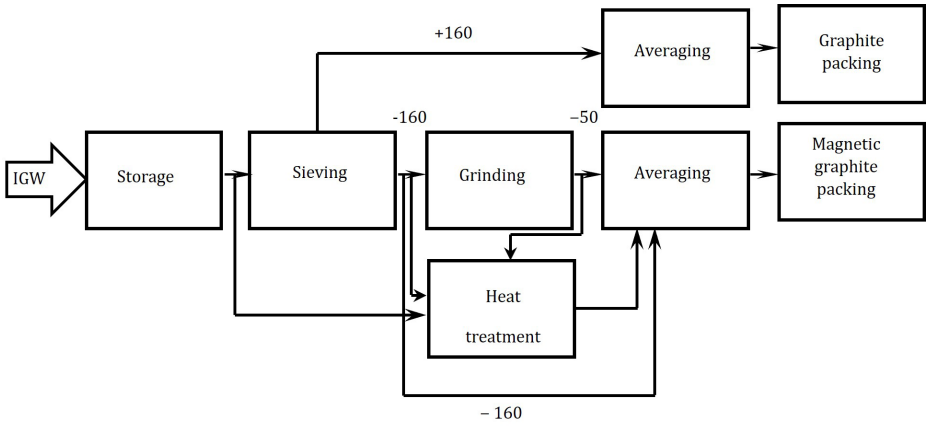

Fig. 13. General scheme of dispersed IGW complex processing, based on [30]

This treatment is the most effective method of increasing the magnetic properties of the starting material and can be done in two ways. The first way is magnetizing annealing, the maximum possible amount of magnetite (Fe_3O_4) in the IGW.

The resulting material can be positioned as "Magnetized magnetic graphite." The second way is reduction processing to metallic iron by carbothermic self-reducing. The resulting material can be characterized as "Metallized magnetic graphite". According to the technological scheme, high-temperature processing can be subjected to both the initial IGW and the product after sieving and milling.

The finished product must have a given level of magnetic and electrical properties. Therefore, the technological scheme provides for averaging the magnetic material's composition.

Thus, a technological scheme with many bonds will make it possible to obtain magnetic graphite with different electrical properties and a practically non-magnetic material containing a large amount of graphite.

The proposed technological scheme was implemented at the Markograph plant (Mariupol, Ukraine) by designing and building a workshop. As a result, fifteen tons of magnetic graphite were produced. Furthermore, from this amount of graphite, 25 tons of composite materials and products for lining rooms with equipment emitting in the microwave range and intended for storing information on electronic media were produced.

An industry standard for magnetic graphite (TU U 02070812.002) was developed.

5. CONCLUSIONS

In this research work, a systematic analysis of the conditions for the formation, structure, and properties of dispersed iron-graphite wastes of metallurgical production was carried out, and ways of their complex utilization were determined. The following was established:

1. The principal amount of dispersed iron-graphite waste at metallurgical enterprises is formed in the desulfurization and mixing departments. Depending on the place of formation, iron-graphite waste contains in its composition a different amount of the main components: carbon, metallic iron, iron oxides, and impurities.
2. Iron-graphite waste is polydisperse. The main number of particles has a size of fewer than 400 microns. The components are unevenly distributed in different fractions of the material. The carbon content decreases from 85% for the fraction (−1000 +200) μm to 7.3% for the fraction less than 50 μm. On the contrary, the total content of iron oxides increases from 7.12% for the fraction (−1000 +200) μm to 78.76% for the fraction less than 50 μm.
3. An analysis of the morphology and microstructure of IGW showed that graphite particles are scaly in shape; iron oxide particles are spherical, a significant part of them are mechanically bonded to graphite, and several particles are even inside graphite flakes.
4. The presence of oxide and metal particles on the surface and inside the graphite plates explains the presence of magnetic properties in iron-graphite waste. At the same time, it was found that the specific saturation magnetization varies depending on the particle size of the material: it increases from 20 $A \cdot m^2/kg$ for a fraction of 200 μm to 50 $A \cdot m^2/kg$ for a fraction of less than 50 μm. The effect of material fineness on the electrical resistivity was also found: ρ_v increases from $(2–6) \cdot 10^{-4}$ ohm·m for particles larger than 200 μm to $5 \cdot 10^3$ ohm·m for particles smaller than 50 μm.
5. Using differential thermal analysis, studies of the temperature conditions for the interaction of iron oxides and graphite in dispersed IGW were carried out. The possibility of magnetizing annealing at 600–700°C and carbothermal self-reduction at temperatures above 980°C has been established.
6. On the basis of studies of the kinetic regularities of magnetizing annealing at various temperatures and modes of motion, the conditions for an almost complete magnetic transformation in dispersed IGW have been established. At a temperature of 650°C, in the combined mode of motion, a material with high electrophysical properties is obtained already in 7 min (σ_s = 87 $A \cdot m^2/kg$, $\rho_v \sim 10^{-4}$ ohm·m).
7. The possibility of obtaining a material with a high specific saturation magnetization (σ_s = 180 $A \cdot m^2/kg$, with a low specific electrical resistance $\rho_v \sim 2 \cdot 10^{-4}$ ohm·m) from dispersed IGW was established by carbothermal self-reduction at a temperature of 1090°C in a combined layer in 24 min.
8. A technological scheme of dispersed IGW processing was proposed and implemented. It provided for two products to be obtained: graphite and magnetic graphite with a given level of electrical and magnetic properties. Tests of magnetic graphite showed its high efficiency both as an independent protective material and as a component of a composite protective material against microwave radiation.

REFERENCES

[1] Pullin H., Bray A.W., Burke I.T., Muir D.D., Sapsford D.J., Mayes W.M. & Renforth P. (2019). Atmospheric Carbon Capture Performance of Legacy Iron and Steel Waste. *Environmental Science & Technology*, 53 (16), 9502–9511. Doi: https://doi.org/10.1021/acs.est.9b01265.

[2] Gurov N.I. & Fedotov A.A. (1982). Opredeleniye ob"yema resursov grafita v grafitosoderzhashchikh otkhodakh metallurgicheskikh zavodov i effektivnost' ikh ispol'zovaniya. *Stal'*, 11, 16–18 [Гуров Н.И., Федотов А.А. (1982). Определение объема ресурсов графита в графитосодержащих отходах металлургических заводов и эффективность их использования. *Сталь*, 11, 16–18].

[3] Fadeyeva N.V., Orekhova N.N. & Gorlova O.Ye. (2019). Opyt pererabotki grafitsoderzhashchey pyli metallurgicheskogo proizvodstva. *Chernaya metallurgiya. Byulleten' nauchno-tekhnicheskoy i ekonomicheskoy informatsii*, 7(5), 632–639. Doi: https://doi.org/10.32339/0135-5910-2019-5-632-639 [Фадеева Н.В., Орехова Н.Н., Горлова О.Е. (2019). Опыт переработки графитсодержащей пыли металлургического производства. *Черная металлургия. Бюллетень научнотехнической и экономической информации*, 7(5), 632–639].

[4] Tolochko A.I., Slavin V.I., Suprun YU.M. & Khayrutdinov R.M. (1990). *Utilizatsiya pyley i shlamov v chernoy metallurgii.* Chelyabinsk: Metallurgiya [Толочко А.И., Славин В.И., Супрун Ю.М., Хайрутдинов Р.М. (1990). *Утилизация пылей и шламов в черной металлургии*. Челябинск: Металлургия].

[5] Laverty P.D., Nicks L.J. & Walters L.A. (1994). *Recovery of Flake Graphite From Steelmaking Kish*. *Report of Investigations 9512.* Reno: United States Department of the Interior Bureau of Mines.
[6] Ozhogin V.V., Tomash A.A. & Chernova S.G. (2003). Polucheniye vysokozakisnogo martenovskogo aglomerata iz otkhodov. *10-ya nauchno-tekhnicheskaya konferentsiya 20–23 maya 2003, Mariupol',* Ukraina, 12–13. Mariupol': Izdatel'stvo PGTU [Ожогин В.В., Томаш А.А., Чернова С.Г. (2003). Получение высокозакисного мартеновского агломерата из отходов. *10*-я научно-техническая конференция *20–23 мая 2003,* Мариуполь, *Украина*, 12–13. Мариуполь: Издательство ПГТУ].
[7] Kravets' V.A. (2018). Doslidzhennya vlastyvostey metalurhiynoho hrafitu z metoyu podal'shoyi utylizatsiyi. *Zbirnyk naukovykh prats' Donbas'koyi natsional'noyi akademiyi budivnytstva i arkhitektury*, 11(1), 38–52. Retrieved from: http://nbuv.gov.ua/UJRN/zbnpdnaba_2018_1_8 [accessed 26.09.2022] [Кравець В.А. (2018). Дослідження властивостей металургійного графіту з метою подальшої утилізації. *Збірник наукових праць Донбаської національної академії будівництва і архітектури,* 11(1), 38–52].
[8] Vertman A.A. & Samarin A.M. (1969). *Svoystva rasplavov zheleza*. Moskva: Nauka[Вертман А.А., Самарин А.М. (1969). *Свойства расплавов железа*. Москва: Наука].
[9] D'yachko Yu.P. & Shaynovich O.I. (1970). Sravneniye razlichnykh skhem podachi zhidkogo chuguna v staleplavil'nyye pechi. *Stal'*, 7, 650–654 [Дьячко Ю.П., Шайнович О.И. (1970). Сравнение различных схем подачи жидкого чугуна в сталеплавильные печи. *Сталь*, 7, 650–654].
[10] Zakharchenko E.V. & Loper K.D. (1981). *Ginezis i morfologiya spelevogo grafita v chugune domennoy plavki. Novoye v metallografii chuguna.* Kiyev: IPL AN USSR [Захарченко Э.В., Лопер К.Д. (1981). *Гинезис и морфология спелевого графита в чугуне доменной плавки. Новое в металлографии чугуна*. Киев: ИПЛ АН УССР].
[11] Tul'chinskiy L.N. (1984). Osobennosti magnitnykh izmereniy poroshkov. In: Tul'chinskiy L.N. (Ed.), *Poroshkovyye magnitnyye materialy*. Kiyev: IPM AN USSR, 117–127 [Тульчинский Л.Н. (1984). Особенности магнитных измерений порошков. В Тульчинский Л.Н., *Порошковые магнитные материалы*. Киев: ИПМ АН УССР, 117–127].
[12] Maslov V.A., Trofimova L.A. & Dan L.A. (2015). Sravneniye fiziko-khimicheskikh svoystv dispersnykh ZHGO miksernogo otdeleniya i otdeleniya desul'furatsii. Teplo- i massoobmennyye protsessy v metallurgicheskikh sistemakh. Materialy IX Mezhdunarodnoy nauchno-tekhnicheskoy konferentsii, Mariupol', Ukraina 9–11 sentyabrya 2015 g. Mariupol': Izdatel'stvo PGTU, 151–155 [Маслов В.А., Трофимова Л.А., Дан Л.А. (2015). Сравнение физико-химических свойств дисперсных ЖГО миксерного отделения и отделения десульфурации. Тепло- и массообменные процессы в металлургических системах. Материалы IX Международной научно-технической конференции, Мариуполь, Украина 9–11 сентября 2015 г. Мариуполь: Издательство ПГТУ, 151–155].
[13] Maslov V.A., Trofimova L.A. & Dan L.A. (2009). Structural-Morphological and Electrophysical Characteristics of Disperse Iron–Graphite Metallurgical Wastes. *Steel in Translation*, 9(7), 551–555. Doi: https://doi.org/10.3103/S0967091209070080.
[14] Shuya Li, Bo Zhang, Di Wu, Zhiwei Li, Sheng-Qi Chu, Xiang Ding, Xingfu Tang, Jianmin Chen & Qing Li (2021) Magnetic Particles Unintentionally Emitted from Anthropogenic Sources. Iron and Steel Plants. *Environmental Science & Technology Letters*, 8, 295–300. Doi: https://doi.org/10.1021/acs.estlett.1c00164.
[15] Michalik J.M., Wilczyńska-Michalik W., Gondek Ł., Tokarz W., Żukrowski J., Gajewska M. & Michalik M. (2022). *Magnetic fraction of the atmospheric dust in Kraków – physicochemical characteristics and possible environmental impact*. Retrieved from: https://doi.org/10.5194/egusphere-2022-462 (accessed 4.07.2022).
[16] Yuzhakov B.A. & Maslov V.A. (1998). Issledovaniye fiziko–khimicheskikh i tekhnologicheskikh svoystv dispersnykh zhelezografitovykh otkhodov OAO «Azovstal'». *Vestnik PGTU*, 6, 30–34 [Южаков Б.А., Маслов В.А. (1998). Исследование физико–химических и технологических свойств дисперсных железографитовых отходов ОАО «Азовсталь». *Вестник ПГТУ*, 6, 30–34].
[17] Berg L.G. (1969). *Vvedeniye v termografiyu*. Moskva: Nauka [Берг Л.Г. (1969). *Введение в термографию*. Москва: Наука].
[18] Shapovalov A.N. (2015). *Teoriya metallurgicheskikh protsessov.* Novotroitsk: NF NITU [Шаповалов А.Н. (2015). *Теория металлургических процессов*. Новотроицк: НФ НИТУ].
[19] Vanyukov A.V. & Zaytsev V.Ya. (1973). Teoriya pirometallurgicheskikh protsessov. Moskva: Metallurgiya [Ванюков А.В., Зайцев В.Я. (1973). *Теория пирометаллургических процессов*. Москва: Металлургия].
[20] Linchevskiy B.V. (1995). *Teoriya metallurgicheskikh protsessov.* Metallurgiya: Moskva [Линчевский Б.В. (1995). *Теория металлургических процессов.* Металлургия: Москва].
[21] Luk'yanchikov A.S. (1962). Gazovyy obzhig zheleznykh rud. Kiyev: Gosudarstvennoye izdatel'stvo tekhnicheskoy literatury [Лукьянчиков А.С. (1962). *Газовый обжиг железных руд*. Киев: Государственное издательство технической литературы].
[22] Lepilo N.N. & Shur A.B. (2000). Modelirovaniye izmeneniy pryamogo vosstanovleniya zheleza v domennoy plavke. Izvestiya VUZov. *Chernaya metallurgiya*, 3, 14–16 [Лепило Н.Н., Шур А.Б. (2000). Моделирование изменений прямого восстановления железа в доменной плавке. Известия ВУЗов. *Черная металлургия,* 3, 14–16].
[23] Zaytsev A.K., Krivolapov N.V., Valavin V.S. & Vandar'yev S.V. (2002). Osobennosti vosstanovleniya zheleza kamennougol'nymi i grafitovymi materialami iz malozhelezistogo shlaka. Izvestiya VUZov. Chernaya metallurgiya, 3, 6–15 [Зайцев А.К., Криволапов Н.В., Валавин В.С., Вандарьев С.В. (2002). Особенности восстановления железа каменноугольными и графитовыми материалами из маложелезистого шлака. *Известия ВУЗов. Черная металлургия*, 3, 6–15].
[24] Trofimova L.O. (2007). Rozrobka tekhnolohiyi vysokotemperaturnoyi pererobky dyspersnykh zalizohrafitovykh vidkhodiv metalurhiynoho vyrobnytstva. Avtoreferat dysertatsiyi na zdobuttya naukovoho stupenya kandydata tekhnichnykh nauk PDTU, Mariupol', Ukrayina [Трофімова Л.О. (2007). *Р*озробка технології високотемпературної переробки дисперсних залізографітових відходів металургійного виробництва. Автореферат дисертації на здобуття наукового ступеня кандидата технічних наук. ПДТУ, Маріуполь, Україна].
[25] Maslov V.A., Trofimova L.A., & Dan L.A. (2006). Dinamika dvizheniya i nagreva dispersnykh zhelezografitovykh otkhodov v gravitatsionno-padayushchem sloye. *Vestnik PGTU*, 16, 1–5. [Маслов В.А., Трофимова Л.А., Дан Л.А. (2006). Динамика движения и нагрева дисперсных железографитовых отходов в гравитационно-падающем слое. *Вестник ПГТУ*, 16, 1–5].
[26] Maslov V.A. & Trofimova L.A. (2004). Issledovaniye kinetiki karbotermicheskogo samovosstanovleniya zhelezografitovykh otkhodov metallurgicheskogo proizvodstva. *Vestnik PGTU*, 14, 41–43 [Маслов В.А., Трофимова Л.А. (2004). Исследование кинетики карботермического самовосстановления железографитовых отходов металлургического производства. *Вестник ПГТУ*, 14, 41–43].
[27] Krylov O.V. (1973). Razvitiye sovremennykh predstavleniy o kinetike geterogennykh reaktsiy v rabotakh S.Z. Roginskogo. Problemy kinetiki i kataliza. XV. Mekhanizm i kinetika geterogennykh reaktsiy. Moskva: Nauka, 5–11 [Крылов О.В. (1973). Развитие современных представлений о кинетике гетерогенных реакций в работах С.З. Рогинского. Проблемы кинетики и катализа. XV. Механизм и кинетика гетерогенных реакций. Москва: Наука, 5–11].
[28] Rozovskiy A.Ya. (1974). *Kinetika topokhimicheskikh reaktsiy.* Moskva: Khimiya [Розовский А.Я. (1974). *Кинетика топохимических реакций*. Москва: Химия].
[29] Barret P. (1973). *Cinétique hétérogène*. Paris: Gauthier-Villars.
[30] Maslov V.A., Trofimova L.A. & Dan L.A. (2018). Pererabotka i utilizatsiya zhelezografitovykh otkhodov metallurgicheskogo proizvodstva. *Liteynoye proizvodstvo i metallurgiya*, 90 (1), 96–99. Doi: https://doi.org/10.21122/1683-6065-2018-1-96-99 [Маслов В.А., Трофимова Л.А., Дан Л.А. (2018). Переработка и утилизация железографитовых отходов металлургического производства. *Литейное производство и металлургия*, 90 (1), 96–99.